Ultrasound in Med. & Biol., Vol. 45, No. 3, pp. 710–719, 2019

0301-5629/$ - see front matter

https://doi.org/10.1016/j.ultrasmedbio.2018.11.013

● *Original Contribution*

SCREENING BREAST LESIONS USING SHEAR MODULUS AND ITS 1-MM SHELL IN SOUND TOUCH ELASTOGRAPHY

LEI ZHANG,*,† JINFENG XU,* HUAIYU WU,* WEIYU LIANG,* XIUQIN YE,* HONGTIAN TIAN,* and FAJIN DONG*

* Department of Ultrasound, First Affiliated Hospital of Southern University of Science and Technology, Second Clinical College of Jinan University, Shenzhen Medical Ultrasound Engineering Center, Shenzhen People's Hospital, Shenzhen, China; and † Guangzhou Medical University, Guangzhou, China

(*Received* 21 *May* 2018; *revised* 22 *November* 2018; *in final from* 30 *November* 2018)

Abstract—The aim of the study described here was to screen breast lesions using either or both shear modulus (*G*) and its 1-mm shell (*S*) in sound touch elastography through a retrospective study of 209 consecutive women with breast lesions. The ability of *G* and *S* data to differentiate between malignant and benign lesions was evaluated using the receiver operating characteristic (ROC) curve. The optimal cutoff point, sensitivity, specificity, positive likelihood ratio (LR+) and negative likelihood ratio (LR−) were calculated. Then, the parameters were pooled to determine the area under the summary receiver operating curve (AUSROC). The pooled sensitivity (PSen), pooled specificity (PSpe), pooled LR+ (PLR+), pooled LR− (PLR−) and diagnostic score (DS) were calculated. Pathologic examination results were used as the reference. In total, 209 patients with 155 benign and 54 malignant lesions were enrolled. For G_{max}, G_{mean} and G_{sd}, the cutoff values were 35.15 kPa ($p = 0.0001$), 10.18 kPa ($p = 0.0001$) and 5.18 kPa ($p = 0.0001$), respectively. For S_{max}, S_{mean} and S_{sd}, the cutoff values were 40.94 kPa ($p = 0.001$), 13.12 kPa ($p = 0.0001$) and 7.97 kPa ($p = 0.0001$), respectively. There were no significant differences in G_{min} and S_{min} between benign and malignant lesions. For the pooled six parameters, the PSen, PSpe, PLR+, PLR−, DS and AUSROC were 86% (95% confidence interval: 82%–89%), 82% (80%–85%), 4.90 (4.24–5.68), 0.17 (0.13–0.22), 3.36 (3.00–3.72) and 91% (88–93%), respectively. The *G* and *S* parameters of sound touch elastography could provide valuable data for the evaluation of breast lesions. Additionally, use of multiple parameters or combined use of the six parameters may be more effective in the evaluation of breast lesions. (E-mail: dongfajin@szhospital.com)

Key Words: **Ultrasonography, Elasticity imaging techniques, Sound touch elastography, Shear modulus, Breast cancer, Diagnosis.**

INTRODUCTION

Breast cancer (BC), which is the second leading cause of death in women, is the most common invasive cancer worldwide (Ban and Godellas 2014; Key et al. 2001). Currently, two sensitive diagnostic methods are routinely used in clinical settings to evaluate BC: mammography and ultrasound (US). However, both methods have limitations. Mammography often yields false-negative (FN) results in patients with dense breasts. US has good sensitivity in detecting breast lesions, but it has poor specificity because most solid lesions are benign lesions (Goddi et al. 2012; Saarenmaa et al. 2001).

Elastography, either strain-based or shear wave based, is a US imaging method that could evaluate tissue stiffness *in vivo*, and is used to characterize lesions that have already been detected on US. Several studies have proved the comparable sensitivity and specificity of elastography in the differentiation between malignant and benign breast lesions (Cho et al. 2008, 2012; Iltoh et al. 2006; Yi et al. 2012).

This study focused on the role of sound touch elastography (STE), which is a novel elastographic technique from Resona 7 US equipment (Mindray Medical Solutions, China), through which the lesion parameters

Address correspondence to: Fajin Dong, Department of Ultrasound, First Affiliated Hospital of Southern University of Science and Technology, Second Clinical College of Jinan University, Shenzhen Medical Ultrasound Engineering Center Shenzhen People's Hospital, Shenzhen 518020, China. E-mail: dongfajin@szhospital.com

shear modulus (*G*, including G_{max}, G_{min}, G_{mean} and G_{sd}) and 1-mm outer shell (*S*, including S_{mean}, S_{max}, S_{min} and S_{sd}) of the lesion can be obtained using the same US device. In the present study, first, we aimed to obtain the aforementioned parameters individually; second, we aimed to obtain the pooled values of these parameters. Finally, we aimed to evaluate the clinical value of using the individual and pooled parameters of STE in the differentiation between malignant and benign breast lesions.

METHODS

Patient selection

This retrospective study was approved by the institutional review board of our hospital. All of the patients enrolled in this study from July 2016 to February 2018 provided informed consent. The results of the US assessments of breast lesions and the entire breast were classified using the Breast Imaging Reporting and Data System (BI-RADS): category 1 = negative; category 2 = benign; category 3 = probably benign; category 4a = low suspicion; category 4b = moderate suspicion; category 4c = high suspicion; and category 5 = highly suggestive of malignancy (Mendelson et al. 2013). Patients meeting the inclusion criteria were enrolled in the study: (i) Lesions had to be detected on US; (ii) the diameter of lesions must range from 5.00 to 30.00 mm; (3) the lesions must be solid or almost solid (<20% cystic); (4) there must be sufficient breast tissue surrounding lesions at the same depth of the US cross section (at least 3 mm around the lesion); (5) lesions must be classified as BI-RADS category 3, 4a, 4b, 4c or 5; (6) patients must not have undergone an intervention or surgery on lesions before US examination; and (6) surgery or biopsy must have been performed within 1 wk after US examination. In addition, for patients with multiple lesions, the one lesion that best satisfied the inclusion criteria was enrolled.

Image acquisition and interpretation

All US scans were conducted by a radiologist (F.D.) who had more than 10 y of experience in US and 4 y of experience in elastography; the radiologist was blinded to the pathologic results. Resona 7 US equipment with the 11L3U linear array transducer (frequency = 3–11 MHz) and STE software, which can measure the stiffness of regions of interest (ROIs), which were circled by the doctor, were used to obtain *G* and *S*.

Patients were placed in a supine position, so that the upper chest was fully exposed. Ultrasound features—lesion morphology, size, boundary, echoes, color Doppler and BI-RADS categories—were recorded.

For patients who met the inclusion criteria, informed consent was obtained, after which an STE examination of the lesion was performed. First, the examination probe was kept in contact with the skin. Next, the size of the ROI was adjusted so that both the lesion and sufficient surrounding tissue were included in the ROI and the majority of the lesion's longitudinal section was included in the center of the ROI. When the left of the two images was nearly green (area >95%) of ROI, as Figure 1 indicates, an elastographic image of the lesion was acquired and saved. Then, STE images were obtained using the same equipment, the lesions were marked, and the G data (including G_{max}, G_{min}, G_{mean} and G_{sd}) and *S* data (including S_{max}, S_{min}, S_{mean} and S_{sd}) were obtained.

Pathologic diagnoses

All pathologic diagnoses were made by a pathologist who had 10 y of experience in the pathologic analysis of BC samples obtained *via* biopsy or surgery.

Statistical analysis

G data (G_{max}, G_{min}, G_{mean}, G_{sd}) and *S* data (S_{max}, S_{min}, S_{mean}, S_{sd}) of STE were recorded. The true-positive, true-negative, false positive and FN values per method were calculated. The Kruskal–Wallis non-parametric test was used to determine whether there were significant differences in the *G* and *S* data between benign and malignant lesions. The abilities of *G* and *S* to differentiate between malignant and benign lesions were evaluated using the receiver operating characteristic curve (ROC). The optimal cutoff point, sensitivity, specificity, LR+ and LR− were calculated. p values < 0.05 were considered to indicate statistical significance. Then, the parameters were pooled to obtain forest images and areas under the summary ROC (AUSROC) curves (Moses et al. 1993). Pooled sensitivity (PSen), pooled specificity (PSpe), pooled LR+ (PLR+), pooled LR− (PLR−) and diagnostic score (DS) were evaluated. All data were analyzed using Stata 14.0 for Mac (Stata Corp., College Station, TX, USA) and GraphPad Prism 6.0 for Mac (GraphPad Software, Inc., La Jolla, CA, USA).

RESULTS

Between July 2016 and February 2018, 230 patients referred for US scans were enrolled in this study. Ten patients whose lesions were >30 mm in diameter and 11 who were lost to follow-up, and thus for whom no pathologic diagnosis was available, were excluded from this study. Finally, a total of 209 patients were included in this study. The patients' characteristics are summarized in Table 1. Among the 209 patients who were finally enrolled in this study, there were 54 malignant lesions, including 48 invasive ductal carcinomas, 2 invasive lobular carcinomas and 4 ductal carcinomas *in situ*. The

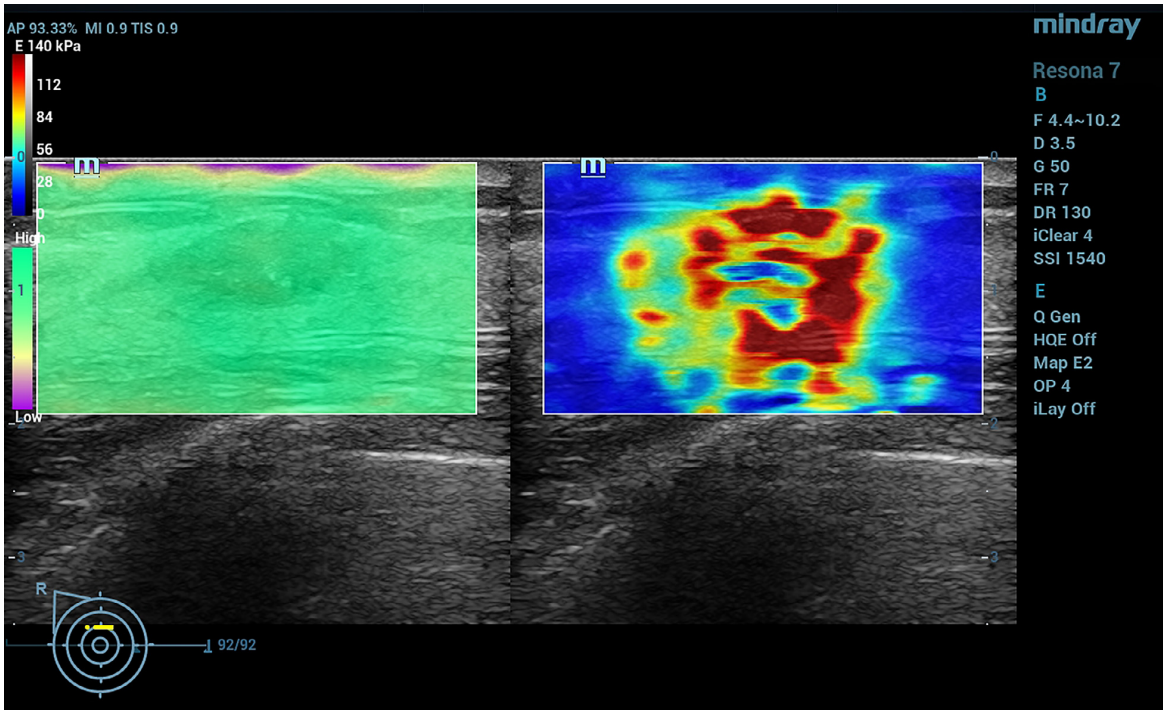

Fig. 1. Before performing the elastography scan, hold the probe still, and keep your hand steady. The images was nearly green of ROI as illustrated.

155 benign lesions included in this study were classified as follows: 138 fibroadenomas, 4 intraductal papillomas, 12 sclerosing adenosis and 1 hamartoma. Analyses were based on cytologic or histologic diagnoses (123 lesions were obtained *via* surgery and 86 *via* biopsy).

G of benign and malignant lesions

Lesion stiffness is illustrated in Figures 2 and 3. The *blue* in the upper left indicates the soft areas of the lesion, and *red* indicates the hard areas of the lesion. In this study, all 54 malignant lesions had a reddish periphery (red rim-like appearance) and were yellow or yellow-green in color in the middle, whereas the 155 benign lesions' color was similar to the surrounding tissues and was either green or yellow in color and no red color was noted, as noted in the malignant lesions.

The *G* data of the benign and malignant breast lesions are summarized in Table 2. G_{max}, G_{mean} and G_{sd} were significantly higher in malignant lesions than in benign lesions ($p < 0.0001$). Their ROC curves are provided in Figure 4. No significant differences in G_{min} were noted between malignant and benign lesions ($p = 0.46$). For G_{max} ($p = 0.0001$), the cutoff, sensitivity, specificity, LR+ and LR− were 35.15 kPa, 87.04%, 82.58%, 5.00 and 0.16, respectively; for G_{mean} ($p = 0.0001$), these values were 10.18 kPa, 81.48%, 80.00%, 4.07 and 0.23, respectively; for G_{sd} ($p = 0.0001$), these values were 5.18, 81.48%, 79.35%, 3.95 and 0.23, respectively. The details are provided in Table 2 and Figure 5.

S data of benign and malignant lesions

Lesion stiffness evaluated with *S* data is indicated with the same color coding system used for the *G* data. The *S* data of benign and malignant breast lesions are outlined in Table 3. For S_{max} ($p = 0.0001$), the cutoff, sensitivity, specificity, LR+ and LR− were 40.94 kPa,

Table 1. Patients' basic information

	No.	Age (y)		Size (mm)	
		Mean	Range	Mean	Range
Benign lesions	155	36.62 ± 10.39	19.00–65.00	13.27 ± 5.61	5.20–30.00
Malignant lesions	54	48.46 ± 13.12	26.00–80.00	19.05 ± 6.14	6.50–29.30

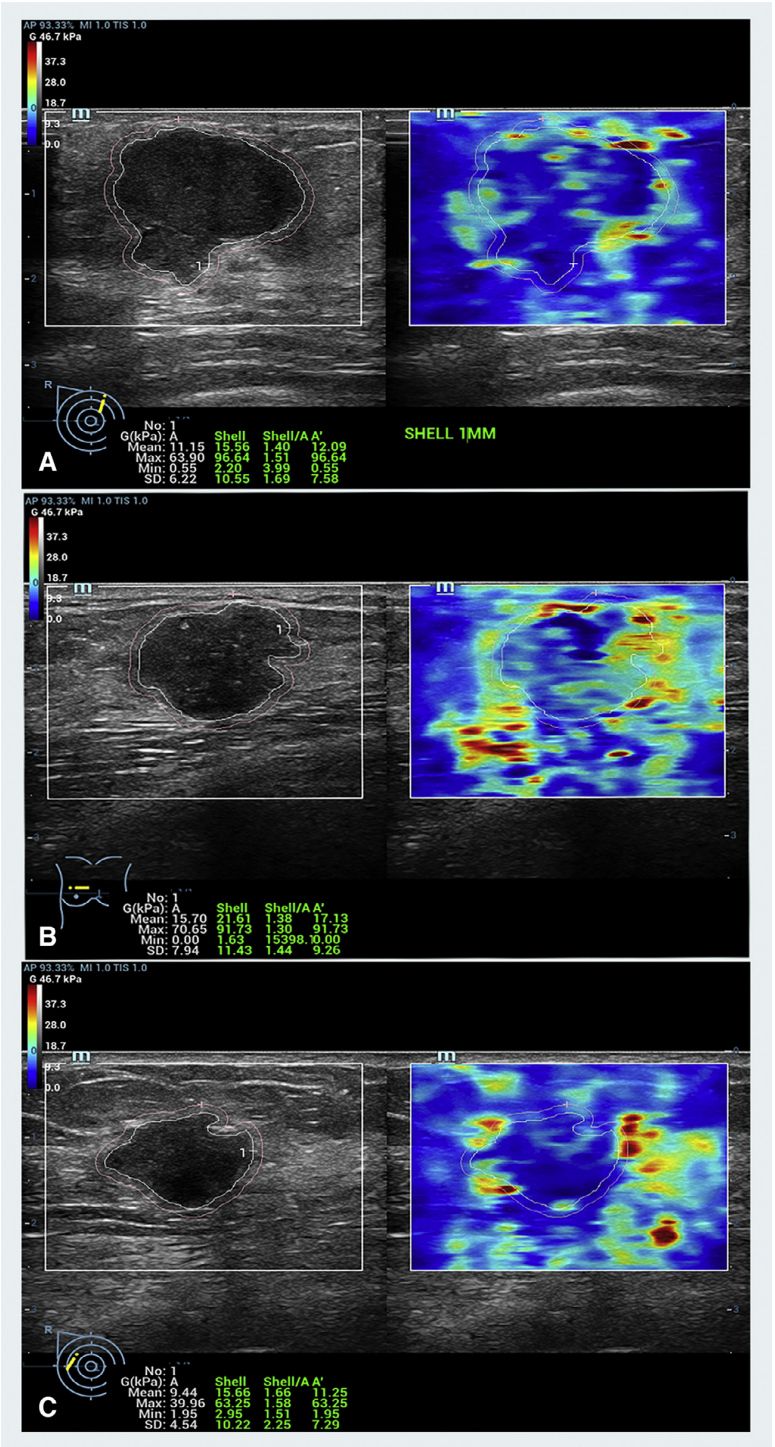

Fig. 2. Sound touch elastography images illustrating *G* and 1.0-mm shell of three invasive ductal carcinoma cases. All images have the "stiff-rim" sign in the peritumoral region. Quantitative parameters were measured by drawing a region of interest around the lesion in the left gray-scale ultrasound image that encompasses the lesion, but does not include the tissue outside the lesion.

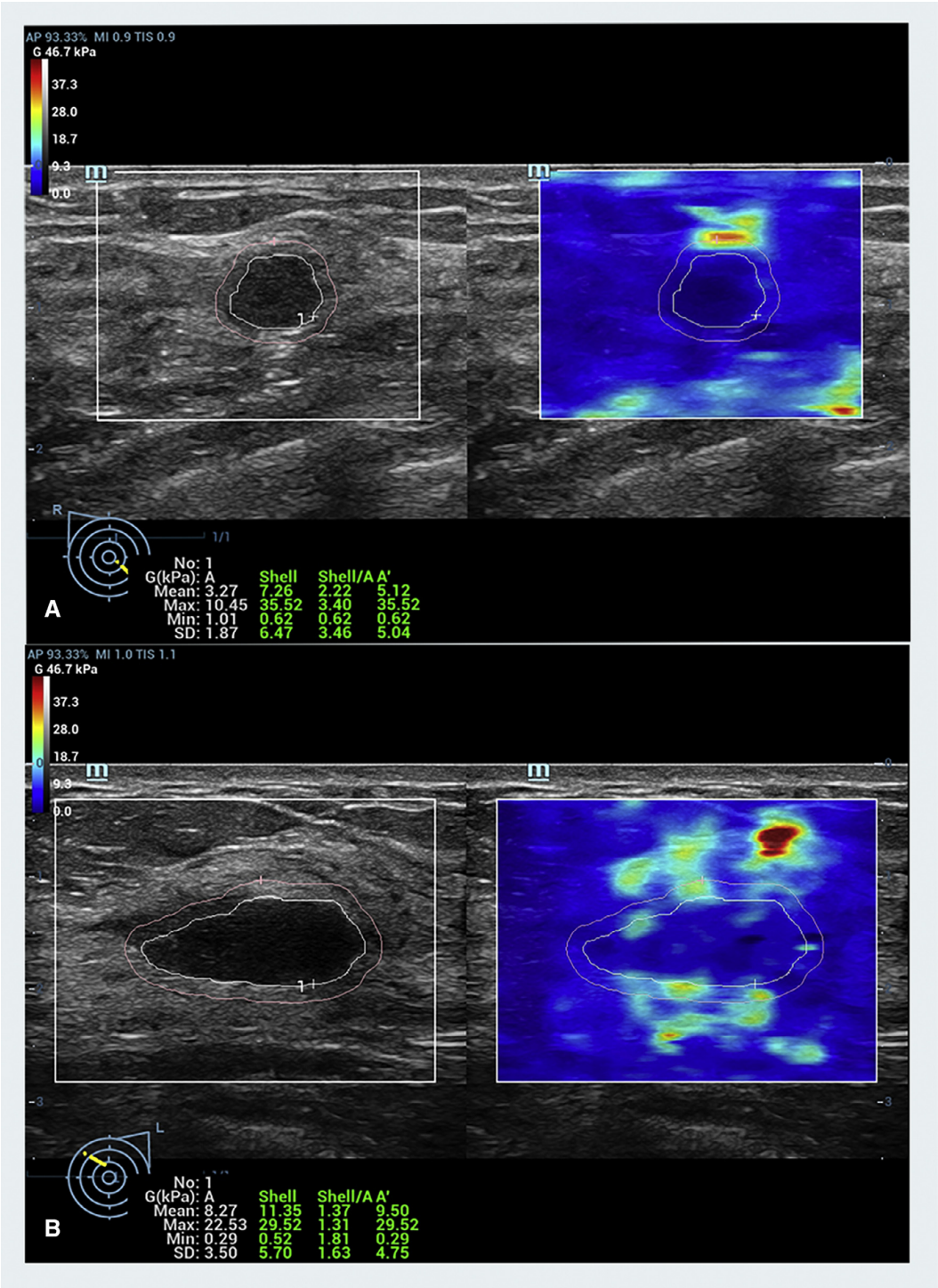

Fig. 3. Sound touch elastography images illustrating *G* and 1.0-mm shell of two benign lesions. The lesions are the same color as the tissue around the lesions. Quantitative parameters were measured by drawing a region of interest around the lesion in the left gray-scale ultrasound image that encompasses the lesion, but does not include the tissue outside of the lesion. (a) Fibroadenoma. (b) Sclerosing adenosis.

Table 2. G measurements of benign and malignant nodules

	Lesion	MAX	MIN	Mean ± SD	*p*	Cutoff	AUC	SEN	SPE	LR+	LR−
G_{mean}	Benign	32.27	1.50	7.87 ± 0.42	0.0001	10.18	82.43%	81.48%	80.00%	4.07	0.23
	Malignant	36.57	4.05	14.77 ± 0.99							
G_{max}	Benign	115.95	3.75	24.19 ± 1.69	0.0001	35.15	89.64%	87.04%	82.58%	5.00	0.16
	Malignant	133.27	10.06	70.29 ± 4.33							
G_{sd}	Benign	17.56	0.51	3.68 ± 0.25	0.0001	5.18	87.13%	81.48%	79.35%	3.95	0.23
	Malignant	22.03	1.72	9.55 ± 0.66							

AUC = area under the receiver operating characteristic curve; LR+ = positive likelihood ratio; LR− = negative likelihood ratio; SD = standard deviation; SEN = sensitivity; SPE = specificity.

88.89%, 83.87%, 5.51 and 0.13, respectively; for S_{mean} ($p = 0.0001$), these were 13.12 kPa, 85.19%, 84.52%, 5.50 and 0.18, respectively; for S_{sd} ($p = 0.0001$), these values were 7.97 kPa, 85.19%, 84.52%, 5.50 and 0.18, respectively. There were no significant differences in S_{min} between benign and malignant lesions. The details are given in Table 3 and Figure 5.

The six parameters of *G* and *S* were pooled together using the Midas module of Stata 14.0, which is equipped with the bivariate mixed-effects regression model developed by van Houwelingen, modified for the synthesis of diagnostic test data (Mendelson et al. 2013; van Houwelingen et al. 2002). For the pooled use of these parameters, PSen, PSpe, PLR+, PLR−, DS and AUSROC were 86% (95% confidence interval: 82%−89%), 82% (80%−85%), 4.90 (4.24−5.68), 0.17 (0.13−0.22), 3.36 (3.00−3.72) and 91% (88%−93%), respectively.

DISCUSSION

'Generally, normal, benign and malignant tissues differ in terms of stiffness; for example, many cancers, such as BC, manifest as extremely stiff lesions (Anderson 1953; Sarvazyan et al. 1995; Walz et al. 1993). Invasive BCs are stiffer than normal tissue and most benign lesions (de Faria Castro Fleury et al. 2009); during the invasive growth of BC, an increase in the stiffness of the surrounding tissue may mean that cancer cells are invading the tissue surrounding the tumor (Iltoh et al. 2006). The internal necrotic area is softer than the outer part of the lesion, which is why the "stiff-rim" sign is seen (Zhou et al. 2014). A previous study had reported that tumor tissue infiltration around the tumor is an independent prognostic factor for predicting tumor recurrence and mortality (De Mascarel et al. 1998). Although these factors cannot be measured directly, elastography is a US technique that can evaluate tissue stiffness indirectly, especially in superficial organs, such as the breast and thyroid. To date, several elastographic methods have been useful in differentiating between benign and malignant breast lesions (Chang et al. 2011; Cosgrove et al. 2012; Feldmann et al. 2015; Leong et al. 2010). STE is a new elastographic imaging method, which can provide both *G* and *S* data of a lesion; the *G* data evaluate the lesion's stiffness, whereas the *S* data evaluate the outer 1 mm of the lesions seen on the US image; thus, the *S* data can help to identify the "stiff-rim" sign in elastography.

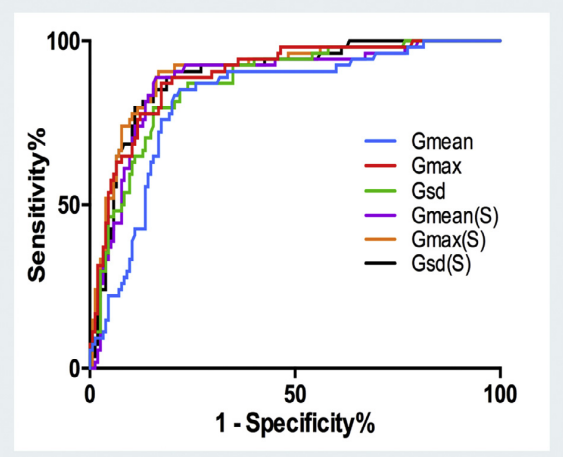

Fig. 4. Multi-receiver operating characteristic analysis of *G* and *S* of malignant and benign breast lesions.

In this study, we evaluated 209 breast lesions (including 155 benign and 54 malignant lesions); six parameters (G_{mean}, G_{max}, G_{sd}, S_{mean}, S_{max} and S_{sd}) proved to be useful in breast lesion evaluation. When these parameters were evaluated individually, the value of these six parameters in distinguishing between benign and malignant breast lesions was ranked as follows: $S_{max} > G_{max} > S_{sd} > S_{mean} > G_{sd} > G_{mean}$; the sensitivity and specificity of all of the aforementioned parameters were greater than 80%. The most optimal parameter was S_{max}. For S_{max}, the cutoff, sensitivity, specificity, LR+ and LR− were 40.94 kPa, 88.89%, 83.87%, 5.51 and 0.13, respectively, compared with those of G_{max}, whose corresponding values were 35.15 kPa, 87.04%, 82.58%, 5.00 and 0.16, respectively. The necrosis of lesions averaging the index, which made the diagnostic value of G_{mean} and S_{mean} were lower than that of G_{max} and S_{max}.

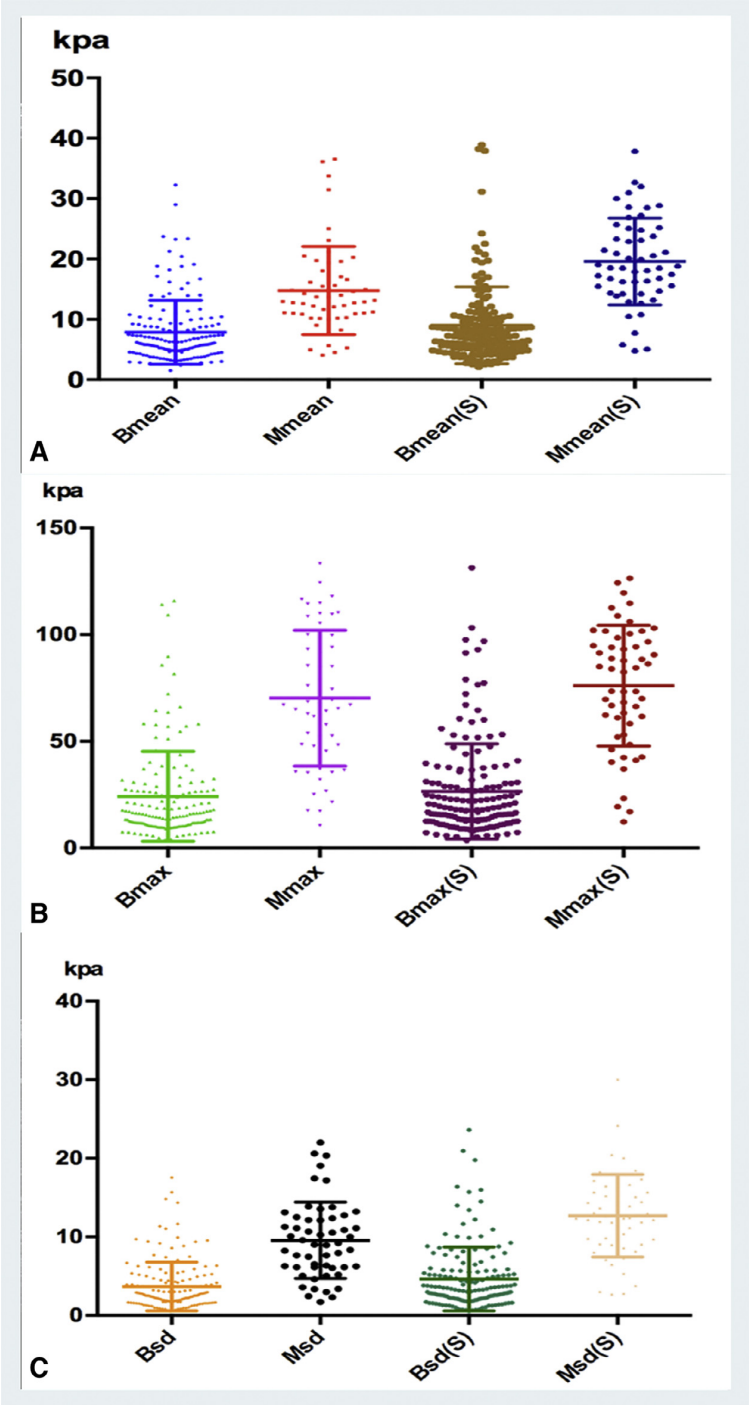

Fig. 5. Distribution of G and S of malignant and benign breast lesions. (A) Mean parameters of G and S. $B_{mean} = G_{mean}$ of benign lesions; $M_{mean} = G_{mean}$ of malignant lesions; $B_{mean}(S) = G_{mean}$ of benign lesions of 1-mm shell; Mean$(S) = G_{mean}$ of malignant lesions of 1-mm shell. (B) Max parameters of G and S. $B_{max} = G_{max}$ of benign lesions; $M_{max} = G_{max}$ of malignant lesions; $B_{max}(S) = G_{max}$ of benign lesions of 1-mm shell; $M_{max}(S) = G_{max}$ of malignant lesions of 1-mm shell. (C) Standard deviation parameters of G and S. $B_{sd} = G_{sd}$ of benign lesions; $M_{sd} = G_{sd}$ of malignant lesions; $B_{sd}(S) = G_{sd}$ of benign lesions of 1-mm shell; $M_{sd}(S) = G_{sd}$ of malignant lesions of 1-mm shell.

Table 3. The 1.0-mm shell of G measurements of benign and malignant nodules

	Lesion	MAX	MIN	Mean ± SD	*p*	Cutoff	AUC	SEN	SPE	LR+	LR−
G_{mean}	Benign	38.88	2.12	9.03 ± 0.51	0.0001	13.12	88.00%	85.19%	84.52%	5.50	0.18
	Malignant	36.57	4.05	19.59 ± 0.98							
G_{max}	Benign	131.02	3.30	26.54 ± 1.79	0.0001	40.94	90.57%	88.89%	83.87%	5.51	0.13
	Malignant	133.27	10.06	76.04 ± 3.85							
G_{sd}	Benign	23.60	0.55	4.67 ± 0.33	0.0001	7.97	89.48%	85.19%	84.52%	5.50	0.18
	Malignant	22.03	1.72	12.69 ± 0.71							

AUC = area under the receiver operating characteristic curve; LR+ = positive likelihood ratio; LR− = negative likelihood ratio; SD = standard deviation; SEN = sensitivity; SPE = specificity.

Table 4. Results for benign and malignant lesions

Parameter	G_{mean}	G_{max}	G_{sd}	S_{mean}	S_{max}	S_{sd}
True positive	44	47	44	46	48	46
False positive	31	27	32	24	25	24
False negative	6	7	10	8	6	8
True negative	124	128	123	131	130	131

Based on the results of this study, we suggest that in the US evaluation of a BC lesion, evaluation of the peripheral region for the presence of the "stiff-rim" sign is superior to evaluation of the lesion area. Zhou et al. (2014) have indicated that the "stiff-rim" sign has the potential to improve differentiation between malignant and benign breast lesions.

As we noted that when using the parameters individually, G_{sd} had the highest FNs and FPs (Table 4), we believe that the pooled use of the parameters, which includes evaluation of both the lesion area and the outer 1-mm shell of the lesion, may be more effective. When we pooled the six parameters, the PSen, PSpe, PLR+, PLR−, DS and AUSROC were 86%, 82%, 4.90,0.17, 3.36 and 91%, respectively (Figs. 6 and 7); as the pooled use of the six parameters involves the evaluation of both the lesion area and the peripheral area for the "stiff-rim" sign, this method has better diagnostic value in differentiating between malignant and benign breast lesions.

This study has some limitations. First, the sample size was not large. Second, the STE technique can also provide the Young's modulus and shear wave velocity of the ROI, which are also valuable in evaluating breast lesions; these parameters were not analyzed, and should be analyzed in future studies.

CONCLUSIONS

Young's modulus has been used to assess the stiffness of lesions. In our study, the *G* and *S* parameters of STE were used to assess breast lesions; the maximum, mean and standard deviation of *G* and *S* are statistically significant and could provide valuable data for differentiating between benign and malignant breast lesions, as these parameters seem to have a high sensitivity, specificity, LR+, LR− and AUC. In addition, the use of

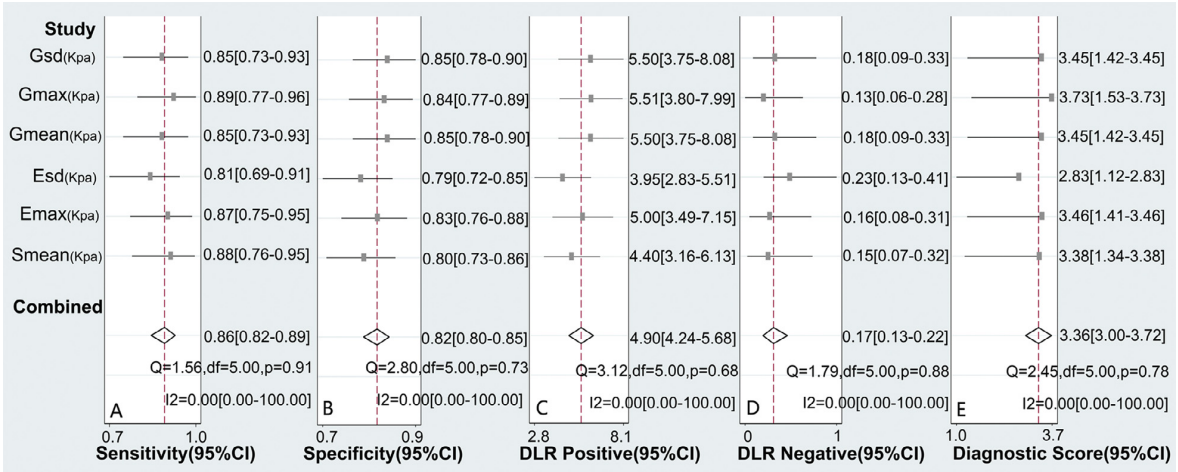

Fig. 6. Pooled sensitivity (s); specificity (b); positive likelihood ratio, LR+ (C); negative likelihood ratio, LR− (D); DOR: diagnostic odds ratio (E) and OR (F) of *G* and *S* with 95% confidence interval (CI), DLR: diagnostic likelihood ratio.

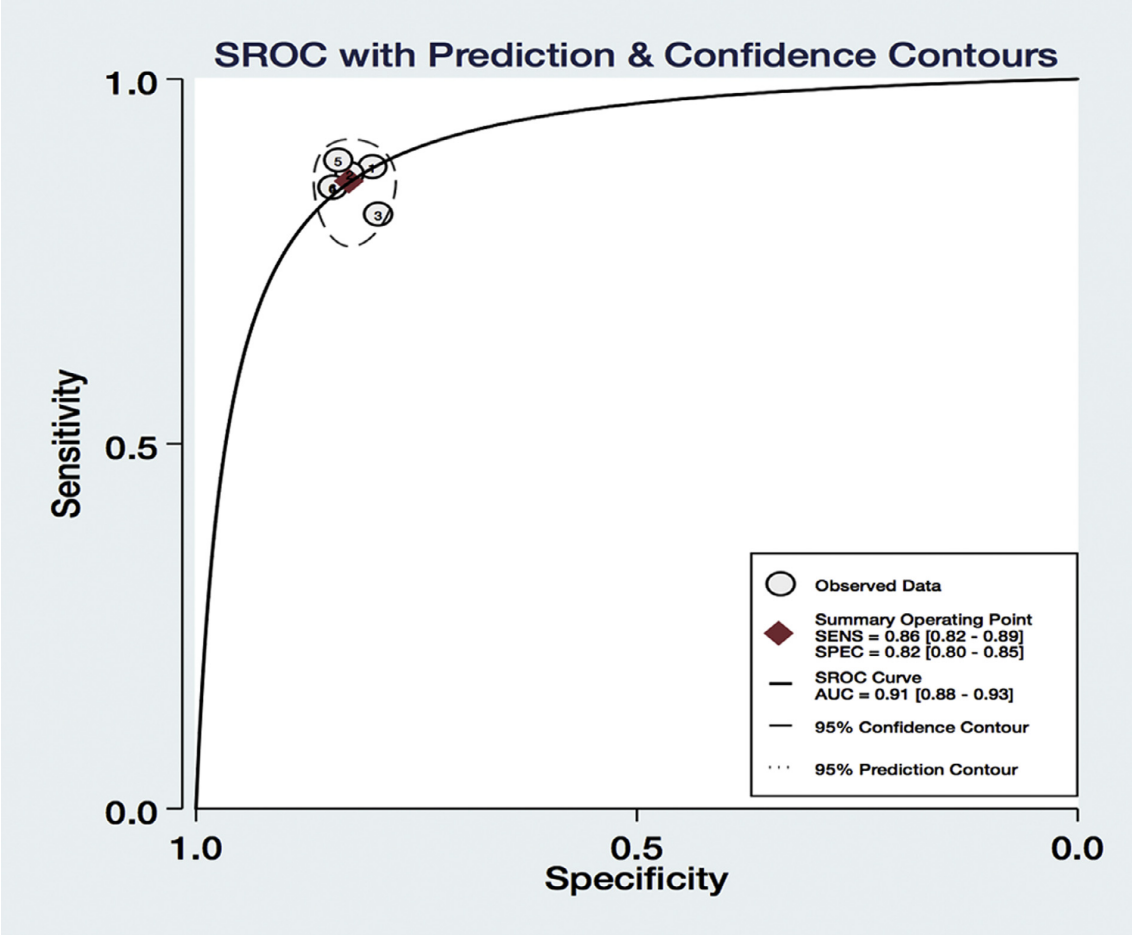

Fig. 7. SROC curves of *G* and *S* (95% confidence interval). AUC: 91% (88%–93%), SENS: 86% (82%–89%); SPEC: 82% (80%–85%). AUC = area under the SROC curve; SENS = sensitivity; SPEC = specificity; SROC = summary receiver operating characteristic curve.

multiple parameters or pooled use of the *G* and *S* parameters may be more effective in evaluating breast lesions. The 1-mm shell could be used to assess the peripheral stiffness of BC and provides a new way to determine BC infiltration.

Acknowledgments—This project was supported by The Clinical Project of Shenzhen People's Hospital (No. SYLY201702).

REFERENCES

Ban KA, Godellas CV. Epidemiology of breast cancer. Surg Oncol Clin North Am 2014;23:409–422.

Chang JM, Moon WK, Cho N, Yi A, Koo HR, Han W, Noh DY, Moon HG, Kim SJ. Clinical application of shear wave elastography (SWE) in the diagnosis of benign and malignant breast diseases. Breast Cancer Res Treat 2011;129:89–97.

Cho N, Moon WK, Park JS, Cha JH, Jang M, Seong MH. Nonpalpable breast masses: Evaluation by US elastography. Korean J Radiol 2008;9:111–118.

Cho N, Jang M, Lyou CY, Park JS, Choi HY, Moon WK. Distinguishing benign from malignant masses at breast US: Combined US elastography and color Doppler US—Influence on radiologist accuracy. Radiology 2012;262:80–90.

Cosgrove DO, Berg WA, Doré CJ, Skyba DM, Henry JP, Gay J, Cohen-Bacrie C. BE1 Study Group. Shear wave elastography for breast masses is highly reproducible. Eur Radiol 2012;22:1023–1032.

de Faria Castro Fleury E, Fleury JC, Piato S, Roveda D, Jr. New elastographic classification of breast lesions during and after compression. Diagn Interv Radiol 2009;15:96–103.

De Mascarel I, Bonichon F, Durand M, Mauriac L, MacGrogan G, Soubeyran I, Picot V, Avril A, Coindre JM, Trojani M. Obvious peritumoral emboli: An elusive prognostic factor reappraised. Multivariate analysis of 1320 node-negative breast cancers. Eur J Cancer 1998;34:58–65.

Feldmann A, Langlois C, Dewailly M, Martinez EF, Boulanger L, Kerdraon O, Faye N. Shear wave elastography (SWE): An analysis of breast lesion characterization in 83 breast lesions. Ultrasound Med Biol 2015;41:2594–2604.

Goddi A, Bonardi M, Alessi S. Breast elastography: Literature review. J Ultrasound Med 2012;15:192–198.

IItoh A, Ueno E, Tohno E, Kamma H, Takahashi H, Shiina T, Yamakawa M, Matsumura T. Breast disease: Clinical application of US elastography for diagnosis. Radiology 2006;239:341–350.

Key TJ, Verkasalo PK, Banks E. Epidemiology of breast cancer. Lancet Oncol 2001;2:133–140.

Leong LC, Sim LS, Lee YS, Ng FC, Wan CM, Fook-Chong SM, Jara-Lazaro AR, Tan PH. A prospective study to compare the diagnostic performance of breast elastography versus conventional breast ultrasound. Clin Radiol 2010;65:887–894.

Mendelson EB, Bohm-Velez M, Berg WA, Whitman GJ, Feldman MI, Madjar H. ACR BI-RADS ultrasound. In: ACR BI-RADS Atlas, Breast Imaging Reporting and Data System. Reston, VA: American College of Radiology; 2013.

Moses LE, Shapiro D, Littenberg B. Combining independent studies of a diagnostic test into a summary ROC curve: Data-analytic approaches and some additional considerations. Stat Med 1993;12: 1293–1316.

Saarenmaa I, Salminen T, Geiger U, Heikkinen P, Hyvärinen S, Isola J, Kataja V, Kokko ML, Kokko R, Kumpulainen E, Kärkkäinen A, Pakkanen J, Peltonen P, Piironen A, Salo A, Talviala ML, Haka M. The effect of age and density of the breast on the sensitivity of breast cancer diagnostic by mammography and ultrasonography. Breast Cancer Res Treat 2001;67:117–123.

van Houwelingen HC, Arends LR, Stijnen T. Advanced methods in meta-analysis: Multivariate approach and metaregression. Stat Med 2002;21:589–624.

Yi A, Cho N, Chang JM, Koo HR, La Yun B, Moon WK. Sonoelastography for 1,786 non-palpable breast masses: Diagnostic value in the decision to biopsy. Eur Radiol 2012;22:1033–1040.

Zhou J, Zhan W, Chang C, Zhang X, Jia Y, Dong Y, Zhou C, Sun J, Grant EG. Breast lesions: Evaluation with shear wave elastography, with special emphasis on the “stiff rim” sign. Radiology 2014;272: 63–72.